EurJIC
European Journal of Inorganic Chemistry

Research Article
doi.org/10.1002/ejic.202300027

Chemistry Europe
European Chemical Societies Publishing

www.eurjic.org

Synthesis and Structural Characterization of Divalent Transition Metal Alkynylamidinate Complexes

Sida Wang,[a] Phil Liebing,[b] Martin Feneberg,[c] Farid M. Sroor,[d] Felix Engelhardt,[a] Liane Hilfert,[a] Sabine Busse,[a] Elias Kluth,[c] Rüdiger Goldhahn,[c] and Frank T. Edelmann*[c]

Dedicated to Professor Hartmut Bärnighausen on the occasion of his 90th birthday.

A series of new alkynylamidinate complexes of selected first and second row transition metals has been synthesized and fully characterized. Treatment of MCl_2 precursors (M=Mn, Fe, Co) with 2 equiv. of the lithium alkynylamidinates Li[*c*-C_3H_5–C≡C–C(NR′$_2$)$_2$]·THF (R′ = ^{i}Pr (2), Cy (cyclohexyl) (**2**)) afforded a series of binuclear complexes of the type M_2[*c*-C_3H_5–C≡C–C-(NR)$_2$-κ*N*:κ*N*′][*c*-C_3H_5–C≡C–C(NR)$_2$-κ^2*N*,*N*′]$_2$ (**3**: M = Mn, R = Cy; **4a**: M = Fe, R = ^{i}Pr; **4b**: M = Fe, R = Cy; **5**: M = Co, R = ^{i}Pr) with no significant metal-metal bonding. In marked contrast, a similar reaction of $CrCl_2$ with 2 equiv. of **1** afforded the homoleptic dinuclear chromium(II) complex Cr_2[*c*-C_3H_5–C≡C–C(N^{i}Pr)$_2$-κ*N*:κ*N*′]$_4$ (**6**) which supposedly comprises a Cr–Cr quadruple bond. Complex **6** could also be prepared in a more rational way and in better yield (61 %) by using dichromium(II) tetraacetate, $Cr_2(OAc)_4$, as starting material. Related reactions employing dimolybdenum(II) tetraacetate, $Mo_2(OAc)_4$, and 2 or 3 equiv. of **1** afforded the mixed-ligand paddle wheel-type complexes *trans*-Mo_2(OAc-κ*O*:κ*O*′)$_2$([*c*-C_3H_5–C≡C–C(N^{i}Pr)$_2$-κ*N*:κ*N*′]$_2$ (**7**) and Mo_2(OAc-κ*O*:κ*O*′)([*c*-C_3H_5–C≡C–C(N^{i}Pr)$_2$-κ*N*:κ*N*′]$_3$ (**8**). All title compounds were structurally characterized through single-crystal X-ray diffraction and spectroscopic techniques (NMR, IR, Raman).

Introduction

The key to influencing the stability, reactivity, and catalytic activity of metal complexes is the fine-tuning of the steric and electronic properties of ancillary ligands attached to the metal centers. This is why tailoring of ligand systems remains in the focus of coordination and organometallic chemists alike.[1–4] In this respect, monoanionic amidinate ligands of the general composition [RC(NR′$_2$)$_2$]$^-$ can be considered nearly ideal ligand systems due to their high degree of variability. Their electronic and steric properties can be modified in a wide range by attaching different substituents at the nitrogen and carbon atoms of the NCN backbone, including the design of unsymmetrically substituted as well as optically active amidinate ligands.[5,6] The amidinate scaffold can even be extended to construct tri- and tetradentate ligand systems by attaching pendant donor groups.[7–11] Over the past three decades, all this has accumulated to a large amidinate ligand library. Consequently, a great variety of homoleptic and heteroleptic amidinate complexes have been synthesized comprising virtually every metallic element ranging from lithium to several actinide metals.[12–17] Notably, bulky amidinate ligands are also suited to stabilize bimetallic chromium and molybdenum complexes containing quadruple and even quintuple bonds.[18–22] The countless possibilities of modifying the ligand backbone make amidinate ligands as versatile as the omnipresent cyclopentadienyl derivatives. Thus it is not surprising that amidinate complexes have come to play important roles in homogeneous catalysis and as volatile precursors in materials science.[1–5]

Alkynylamidinate ligands of the type [R–C≡C–C(NR′$_2$)$_2$]$^-$ are obtained when an alkynyl group (R–C≡C–) is attached to the central carbon atom of an amidinate anion. Certain alkynylamidinate complexes of transition metals and rare-earth metals have already been demonstrated to be excellent catalysts for addition reactions of C–H, N–H and P–H bonds to carbodiimides and also the polymerization of polar monomers (e.g. ε-caprolactone).[23–29] The ligand precursors in the form of lithium alkynylamidinates are easily accessible by deprotonation of terminal alkynes with *n*-butyllithium. Subsequent insertion reactions of 1,3-diorganocarbodiimides (R′–N=C=N–R′) into the Li–C bond of the lithium alkynyl intermediates R–C≡C–Li directly affords the desired lithium

[a] Dr. S. Wang, Dr. F. Engelhardt, Dr. L. Hilfert, Dr. S. Busse
Institut für Chemie,
Otto-von-Guericke-Universität Magdeburg
Universitätsplatz 2, 39106 Magdeburg (Germany)
[b] Dr. P. Liebing
Institut für Anorganische und Analytische Chemie,
Friedrich-Schiller-Universität Jena
Humboldtstr. 8, 07743 Jena (Germany)
[c] Dr. M. Feneberg, E. Kluth, Prof. Dr. R. Goldhahn, Prof. Dr. F. T. Edelmann
Institut für Physik,
Otto-von-Guericke-Universität Magdeburg
Universitätsplatz 2, 39106 Magdeburg (Germany)
E-mail: frank.edelmann@ovgu.de
http://www.ich.ovgu.de/Lehrstühle/Anorganische+Chemie/Prof_+i_R_+Edelmann-p-302.html
[d] Prof. F. M. Sroor
Organometallic and Organometalloid Chemistry Department,
National Research Centre
Cairo 12622 (Egypt)

Supporting information for this article is available on the WWW under https://doi.org/10.1002/ejic.202300027

Research Article
doi.org/10.1002/ejic.202300027

alkynylamidinates as crystalline solids. The entire preparation can be carried out as a one-pot synthesis. Most commonly, the *N*-substituents R′ are *iso*-propyl (^{i}Pr) and cyclohexyl (Cy) because the carbodiimides ^{i}Pr–N=C=N–^{i}Pr and Cy–N=C=N–Cy are commercially available due to their widespread use as coupling reagents in peptide synthesis. Bulky 2,6-diisopropylphenyl (Dipp) substituents on the N atoms have also been successfully utilized.[30] Regarding the substituent at the carbon atom of the NCN backbone, *C*-phenyl- and *C*-trimethylsilyl-alkynylamidinate anions [R–C≡C–C-(NR′)$_2$]$^-$ (R = Ph, SiMe$_3$; R′ = ^{i}Pr, Cy) have been employed most often in previous studies.[23–33] A few years ago we initiated a research project to study the coordination chemistry of alkynylamidinate anions with R = cyclopropyl (*c*-C$_3$H$_5$) in view of the unique electronic properties of the three-membered cyclopropyl ring.[34,35] In the first step the easily accessible lithium cyclopropylethynylamidinate precursors Li[*c*-C$_3$H$_5$–C≡C–C(NR)$_2$]·THF (R = ^{i}Pr, Cy)[36] were prepared and structurally characterized. Further in the course of this study, a surprising variety of transition metal and lanthanide alkynylamidinate complexes terminated by cyclopropyl groups could by synthesized and fully characterized.[37–44] In this contribution we now report the synthesis and characterization of several new first and second row transition metal complexes comprising the cyclopropylethynylamidinate ligands.

Results and Discussion

Synthesis and Characterization

Reactions of transition metal(II) chlorides MCl$_2$ (M = Mn, Fe, Co) with 2 equiv. of the lithium cyclopropylethynylamidinate precursors Li[*c*-C$_3$H$_5$–C≡C–C(NR)$_2$]·THF (R = ^{i}Pr (**1**), Cy (**2**)) were carried out in THF solutions as illustrated in Scheme 1. This produced brightly colored solutions accompanied by precipitation of LiCl. The products were isolated by crystallization from *n*-pentane. The complexes **3** (Mn; yellow), **4a** (Fe; yellow), **4b** (Fe; orange) and **5** (Co; yellow-green) were isolated in moderate yields in the range of 39–59% as air- and moisture-sensitive crystals. Possible reasons for the relatively low isolated yields of pure crystalline materials could be the very high solubility of the compounds even in non-polar hydrocarbon solvents and/or increasing amounts of impurities when working up the mother liquors.

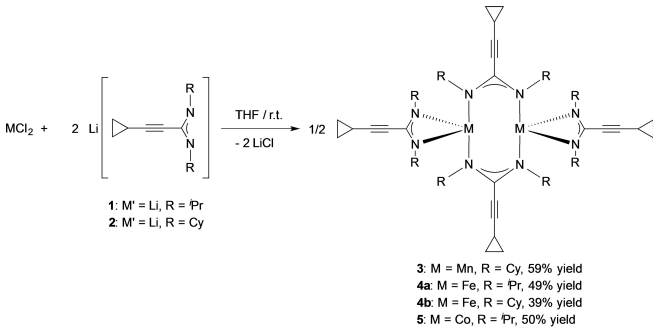

Scheme 1. Preparation of the binuclear alkynylamidinate complexes **3**–**5**.

All four compounds were fully characterized by spectroscopic and analytical methods as well as X-ray diffraction studies. The collected data were consistent with the presence of dinuclear homoleptic species comprising four-coordinate metal ions. The IR spectra of **3**–**5** showed characteristic medium strong bands in the range of 1593–1606 cm^{-1} which can be attributed to the stretching vibration of the NCN units in the ligands.[45] The C≡C bond stretching vibrations were observed as medium bands in the very narrow range of 2218–2225 cm^{-1} in the IR spectra of **3**–**5**, which is consistent with the value reported for the Li precursor **1** (2121 cm^{-1}).[31,36] EI mass spectra of the four complexes did not show the molecular ions but only a few characteristic fragments. The peak at *m/z* 705 in the mass spectrum of **4a** could be assigned to the fragment [*M*−4 ^{i}Pr]$^+$, while the peak at *m/z* 593 in the mass spectrum of **5** corresponds to the fragment [*M*−3^{i}Pr−4(*c*-C$_3$H$_5$)]$^+$. In the case of complexes **3** and **4b**, the peaks at *m/z* 667 and 595 could be assigned to [*M*−3(*c*-C$_3$H$_5$–C≡C)−4Cy]$^+$ and [*M*−2{*c*-C$_3$H$_5$–C≡C–C-(NCy)$_2$}–Cy]+, respectively. The paramagnetic nature of the Mn^{2+}, Fe^{2+} and Co^{2+} ions prevented the measurement of interpretable NMR spectra except for compound **4b** (cf. Experimental Section).

The reaction shown in Scheme 1 was also carried out using anhydrous chromium(II) chloride, CrCl$_2$, and 2 equiv. of **2** as starting materials. The reaction in THF followed by extraction with *n*-pentane and recrystallization from the same solvent afforded beautiful, orange-red, block-like crystals which turned out to be the dinuclear complex Cr$_2$[μ-*c*-C$_3$H$_5$–C≡C–C(N^{i}Pr)$_2$]$_4$ (**6**) for which an X-ray crystal structure determination suggested the presence of a direct Cr–Cr bond (see below). With 41% the isolated yield of compound **6** using CrCl$_2$ as starting material was rather low. This can be traced back to the facts that the complex is not only quite air- and moisture-sensitive but also highly soluble in non-polar solvents such as *n*-pentane. Once the molecular structure of **6** had been established through X-ray diffraction, we set out to establish a more deliberate route starting from dichromium(II) tetraacetate, Cr$_2$(OAc)$_4$, which already contains a Cr–Cr quadruple bond.[46] As expected, treatment of anhydrous Cr$_2$(OAc)$_4$ with 4 equiv. of **1** provided complex **6** in significantly improved yield (60%). Scheme 2 summarizes the different synthetic routes leading to complex **6**. The product was fully characterized by analytical and spectroscopic methods as well as single-crystal X-ray diffraction. The IR spectrum of **6** showed a medium absorption band at 2220 cm^{-1} which could be assigned to the C≡C stretching vibration of the alkynylamidinate ligands,[31,36] while another very strong band observed at 1506 cm^{-1} is attributable to the stretching vibrations of the NCN units in the amidinate ligands.[45] Elemental analysis values for C, H, and N of **22** were in good agreement with the proposed formulation. The molecular ion peak of **6** was observed in the EI mass spectrum at *m/z* 869. The ^{1}H and ^{13}C NMR spectra of **6**

Research Article
doi.org/10.1002/ejic.202300027

Chemistry Europe
European Chemical Societies Publishing

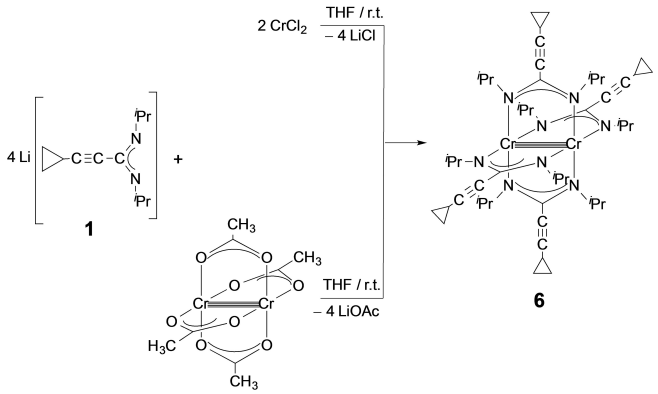

Scheme 2. Different synthetic routes leading to the dichromium(II) complex **6**.

displayed sharp signals typical for a diamagnetic compound, which suggests that a Cr–Cr quadruple bond is present in analogy to $Cr_2(OAc)_4$.[46]

Finally, two new dimolybdenum(II) complexes could be synthesized in a similar manner starting with dimolybdenum(II) tetraacetate, $Mo_2(OAc)_4$.[47] In this case, two different mixed-ligand amidinate-acetate complexes could be prepared depending on the stoichiometric ratio of the reactants. The experimental results are illustrated in Scheme 3. Treatment of $Mo_2(OAc)_4$ with 2 equiv. of **1** provided the 2:2 mixed-ligand paddle wheel-type complex *trans*-$Mo_2(\mu\text{-}OAc)_2[\mu\text{-}c\text{-}C_3H_5\text{–}C{\equiv}C\text{–}C(N^iPr)_2]_2$ (**7**) in rather low isolated yield (30%) in the form of orange, block-like crystals. The same reaction carried out in a 1:3 molar ratio afforded the tris(alkynylamidinate) derivative $Mo_2(\mu\text{-}OAc)[\mu\text{-}c\text{-}C_3H_5\text{–}C{\equiv}C\text{–}C(N^iPr)_2]_3$ (**8**) which also forms orange, block-shaped crystals (40% yield). Once again, the fairly low isolated yields are assumed to be a result of the high solubility of both compounds even in *n*-pentane. Notably, neither a 1:1 nor a homoleptic 1:4 product could be isolated in pure form. Treatment of $Mo_2(OAc)_4$ with 4 equiv. of **1** resulted in the formation of **8** admixed with unreacted **1**. The highly air- and moisture-sensitive complexes were fully characterized in the usual manner by NMR, IR, and Raman spectroscopy, mass spectrometry, as well as elemental analyses. As expected, the IR data did not differ significantly from those of the other transition metal complexes **3**–**6**. Thus the most prominent IR bands could be readily assigned. As was observed in the IR spectra of **3**–**5**, the C≡C triple bond stretching vibrations in the spectra of **6**–**8** were observed in the very narrow range of 2216–2227 cm^{-1}. For all title compounds this means that the C≡C triple bond stretch is not significantly affected by the respective transition metal ions as apparently the alkyne moieties are too far away from the central metals. Gratifyingly, the presence of a short Mo–Mo bond in complexes **7** and **8** could also be verified by Raman spectroscopy. The Raman spectra of **6**–**8** showed clear Raman bands for several different Raman shift ranges (Figure 1). A band at 424 cm^{-1} in the spectra of both dimolybdenum compounds **7** and **8** could be clearly assigned to the Mo–Mo stretch. This is in perfect agreement with the data reported by John et al. for $Mo_2(dmp)_4$ (dmp = 2,6-dimethoxyphenyl).[48] In the Raman spectrum of the dichromium compound **6** no such band was detected, which is also in good agreement with the Raman spectroscopy results reported for $Cr_2(dmp)_4$.[48] All other Raman modes are likely ligand modes modified by the different metal atoms to different extends, i.e. they are present in both Cr and Mo compounds but shifted to slightly different positions.

In the mass spectra of **7** and **8** the molecular ions were clearly observed. Due to the diamagnetic nature of Mo^{2+} in the dimolybdenum(II) complexes **6**–**8**, well-resolved NMR spectra could be obtained which showed a far-reaching similarity with the NMR spectra of the lithium amidinates **1** and **2** (see Experimental Section for details). Notably, the ^{13}C

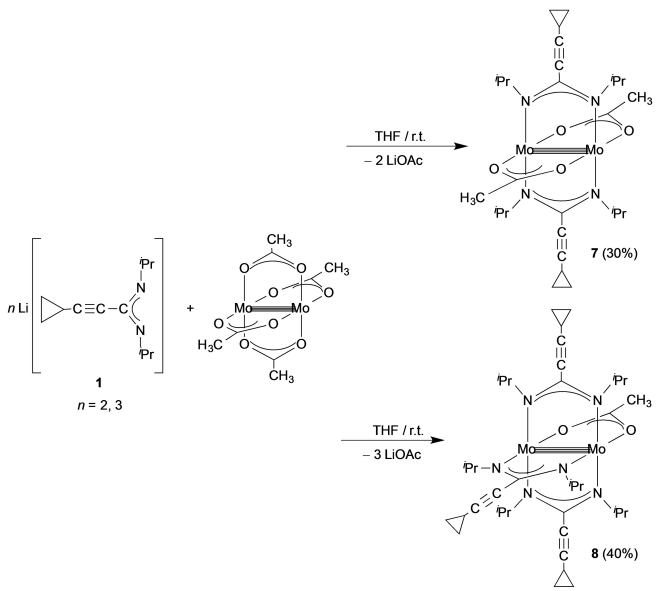

Scheme 3. Synthetic routes leading to the dimolybdenum(II) complexes **7** and **8**.

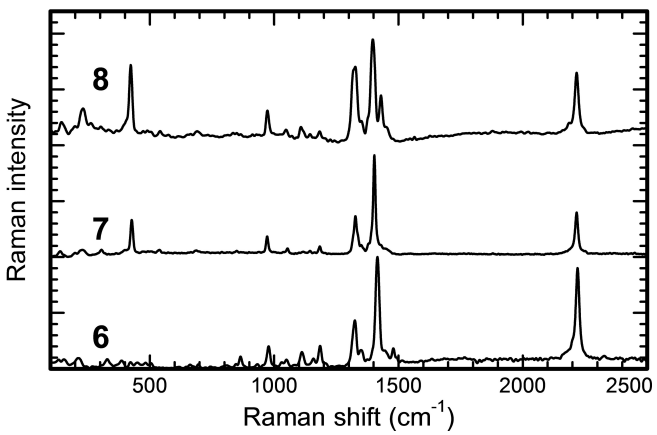

Figure 1. Normalized Raman spectra for compounds **6**–**8** (spectra are vertically shifted for clarity).

Research Article
doi.org/10.1002/ejic.202300027

Table 1. Crystal data and details on structure refinement for the reported compounds.

	3·0.5 *n*-C_6H_{14}	4a	4b	5	6	7
CCDC deposition number	2226417	2226418	2226419	2226420	2226421	2226422
Chemical formula sum	$C_{75}H_{115}Mn_2N_8$	$C_{48}H_{76}Fe_2N_8$	$C_{72}H_{108}Fe_2N_8$	$C_{48}H_{76}Co_2N_8$	$C_{48}H_{76}Cr_2N_8$	$C_{28}H_{44}Mo_2N_4O_4$
Formula weight/g mol^{-1}	1238.62	876.86	1197.36	883.02	869.16	692.55
Crystal color and shape	yellow prism	yellow prism	orange block	yellow-green plate	orange rod	orange block
Crystal system	monoclinic	monoclinic	monoclinic	monoclinic	monoclinic	triclinic
Space group	*C*2/*c*	*C*2/*c*	*C*2/*c*	*C*2/*c*	$P2_1/c$	$P\bar{1}$
Unit cell parameters	43.338(1)	23.2180(8)	42.78(1)	23.1687(7)	11.161(2)	8.881(4)
a (Å)						
b (Å)	16.0374(2)	9.5855(4)	15.921(2)	9.5358(2)	14.170(3)	11.638(4)
c (Å)	22.0688(5)	22.7357(7)	21.913(4)	22.7158(7)	30.435(6)	15.952(6)
α (°)	90	90	90	90	90	85.63(3)
β (°)	113.721(2)	96.321(3)	113.41(2)	96.107(2)	98.34(3)	85.84(4)
γ (°)	90	90	90	90	90	68.22(3)
Unit cell volume/Å^3	14042.4(5)	5029.2(3)	13696(5)	4990.2(2)	4763(2)	1525(1)
Molecules per cell *Z*	8	4	8	4	4	2
Calcd. density ρ/g cm^{-3}	1.172	1.158	1.161	1.175	1.212	1.508
μ (Mo-K_α)/mm^{-1}	0.406	0.615	0.469	0.703	0.497	0.860
Crystal size/mm	0.32×0.26×0.16	0.41×0.28×0.14	0.20×0.20×0.20	0.37×0.18×0.15	0.58×0.52×0.34	0.19×0.16×0.09
T/K	153(2)	153(2)	100(2)	133(2)	100(2)	100(2)
θ range/°	1.996…25.097	2.435…25.997	1.830…25.350	2.447…25.999	1.974…24.999	1.887…28.282
Reflections collected	39331	17383	37825	15518	21907	15009
Reflections unique	12443	4938	12504	4901	8230	7481
Reflections with $I > 2\sigma(I)$	9914	4427	10172	4225	5673	6977
Completeness of dataset	99.4%	99.7%	99.5%	99.8%	97.9%	98.9%
R_{int}	0.0416	0.0274	0.0420	0.0329	0.0499	0.0572
Parameters/Restraints	797/106[a]	270/0	779/1342[a]	270/0	568/30[a]	399/612[a]
R_1 (all data/$I > 2\sigma(I)$)	0.0667/0.0488	0.0333/0.0280	0.0554/0.0402	0.0377/0.0296	0.0961/0.0647	0.0436/0.0397
wR_2 (all data/$I > 2\sigma(I)$)	0.1269/0.1184	0.0670/0.0649	0.0863/0.0817	0.0710/0.0680	0.1523/0.1441	0.0949/0.0930
goodness-of-fit on F^2	1.036	1.055	1.013	1.028	1.114	1.197
Largest diff. peak and hole/e Å^{-3}	0.771/−0.680	0.281/−0.253	0.303/−0.354	0.232/−0.338	0.830/−0.670	0.689/−1.009

[a] Restraints on the disordered groups (SADI, SIMU, RIGU, EXYZ, EADP).

NMR spectrum of **8** displays two sets of signals for every amidinate carbon atom of the amidinate, thus reflecting the *cis*- and *trans*-positioned alkynylamidinate ligands with respect to the acetate ligand. Notably, the NMR signals for both **7** and **8** are very sharp, which is in agreement with the expected presence of a Mo–Mo quadruple bond and the consequent diamagnetic nature of both compounds.

Solid-State Molecular Structures

All new complexes reported here show a high tendency to crystallize, so that single-crystals of compounds **3**–**5** could easily be grown by cooling saturated solutions in *n*-pentane (**4a**, **4b**, **5**) or *n*-hexane (**3**) to 5 °C for several days. The crystallographic data for the title compounds are listed in Table 1. The X-ray studies confirmed the presence of homoleptic, four-coordinate dimers in which the metal atoms are both coordinated by one κ^2N,N'-chelating alkynylamidinate ligand and two $\kappa N{:}\kappa N'$-bridging alkynylamidinate ligands, resulting in the formation of twisted eight-membered $M_2C_2N_4$ rings.

Since the structures are all very similar, only the molecular structures of the iron(II) derivatives **4a** and **4b** are depicted in Figures 2 and 3 as typical examples of *iso*-propyl- and cyclohexyl-substituted derivatives (cf. Figures S21 and S22 in the Supporting Information for **3** and **5**). A notable difference between these two derivatives is that **4a** shows crystallographically imposed C_2 symmetry, whereas in **4b** the two parts of the molecule are not symmetry-related. One of the two bridging amidinate moieties is significantly twisted around the *c*-C_3H_5–C≡C– vector, so that the Fe–N distances to the opposite N atoms are strongly reduced (Fe1···N3 and Fe2···N4, respectively).

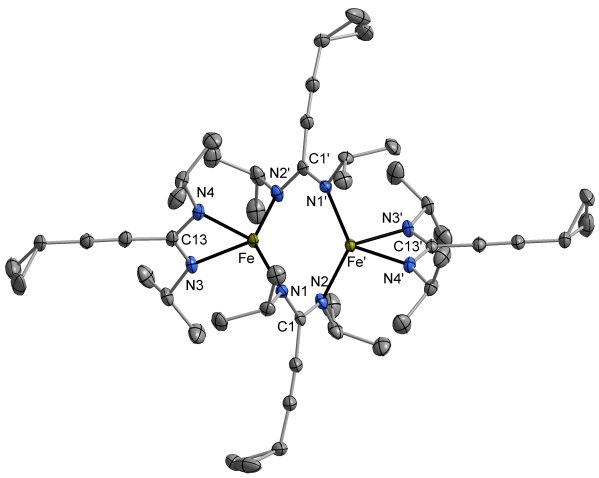

Figure 2. Molecular structure of compound **4a** in the crystalline state. Displacement ellipsoids with 40% probability, H atoms omitted for clarity. The molecule exhibits crystallographically imposed C_2 symmetry. Symmetry code to generate equivalent atoms: ′−x, y, 0.5−z.

Research Article
doi.org/10.1002/ejic.202300027

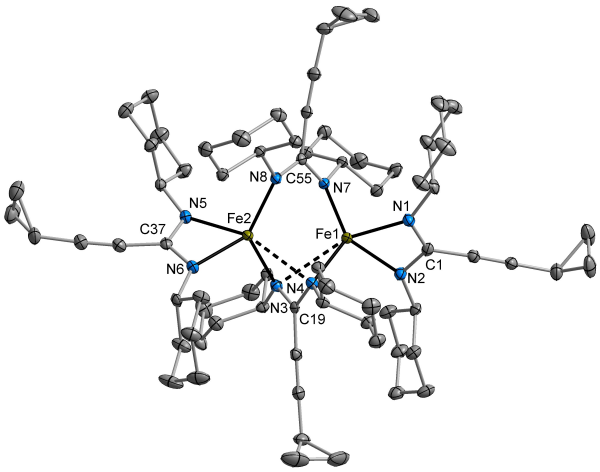

Figure 3. Molecular structure of compound **4b** in the crystalline state. Displacement ellipsoids with 50% probability, H atoms and disorder of an alkynyl backbone omitted for clarity.

In general, and as expected, the M–N bond lengths in the molecular structures of compounds **3**–**5** are proportional to the ionic radii of the metals ($Mn^{2+} > Fe^{2+} > Co^{2+}$). Also regarding the M–N bond lengths there are two significant trends which can be observed. First of all, the M–N-distances to the terminal amidinate moieties are generally somewhat longer than those to the bridging ones. For example, in complex **4a** the average Fe–N bond length to the bridging amidinate ligands is 2.058(1) Å, which is slightly shorter than that observed in the terminal chelating ligand (2.110(1) Å). Comparing the Fe–N bond lengths in two iron(II) bis(amidinate) complexes **4a** and **4b**, they are slightly elongated by the substituent at the nitrogen atoms in the NCN units when going from *iso*propyl to cyclohexyl groups [**4a**: 2.109(1), 2.058(1) Å; **4b**: 2.168(2), 2.063(2) Å. Apparently a bulkier substituent at nitrogen in the NCN units of amidinate moiety leads to longer M–N bond lengths. With a range of 2.047(1) to 2.150(2) Å, the Fe–N bond lengths are in good agreement with those reported for the related iron bis(amidinate) complex $Fe_2(DPhBz)_4$ (DPhBz = diphenylbenzamidinate anion) where the Fe–N distances are in the range of 2.065(3) to 2.186(3) Å.[49] The coordination environment around the iron atoms in **4a** can be described as a distorted tetrahedral arrangement which is characterized by the angles N(1)–Fe–N(3) 104.8(5), N(2′)–Fe–N(1) 132.8(1), N(3)–Fe–N(4) 69.9(1), N(4)–Fe–N(2′) 105.7(1)°, respectively. The coordination around the Fe atoms in **4a** is illustrated in Figure 4 (as a typical representative of the series). As expected, a very similar coordination environment of the metal atoms is found in the other three complexes **3**, **4b**, and **5**. The relatively long Fe–Fe distance of 3.001(6) Å in **4a** as compared to 2.462(2) Å found in the $Fe_2(DPhF)_4$ (DPhF = *N,N′*-diphenylformamidinate anion) indicates that there is no Fe–Fe bond present in this dimer; a similar observation (3.124(1) Å) was also made in the analogous iron bis(amidinate) complex $Fe_2(DPhBz)_4$.[49] Similarly, the M···M distances in the complexes **3**, **4b**, and **5** are also rather long and outside the bonding range [**3**: 3.161(5), **4b**: 3.072(6), **5**: 3.057(4) Å].

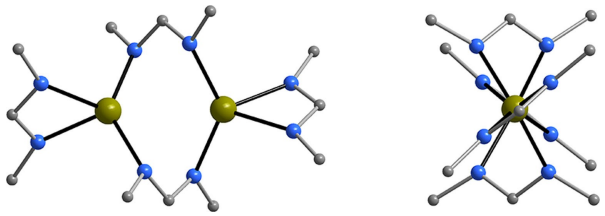

Figure 4. Representation of the coordination sphere of the Fe atoms in compound **4a** viewed perpendicularly to (left) and along the Fe–Fe vector (right).

Single-crystals of the dichromium(II) compound **6** were also obtained by cooling a concentrated solution in *n*-pentane to 5 °C. The complex crystallizes in the monoclinic space group $P2_1/c$ with one molecule in the asymmetric unit. Figure 5 shows the well-known paddle-wheel structure, which is a typical arrangement of quadruply bonded dinuclear $Cr_2(amidinate)_2$ molecules. The molecular structure of **6** is formed by a Cr–Cr unit bridged by four κ*N*:κ*N′*-cyclopropylethinylamidinate groups. Consequently, each Cr atom is bonded to four N atoms of four amidinate ligands, and each of the two donor atoms of a amidinate ligand is combined with two Cr centers to form a five-membered ring. The Cr–N bond lengths [Cr(1)–N(1) 2.078(4), Cr(1)–N(3) 2.043(4), Cr(1)–N(5) 2.070(4), Cr(1)–N(7) 2.046(4) Å] are typical and compare well for example with those of the previously reported quadruply bonded dichromium complex $Cr_2[HC(NCy)_2]_4$ (2.03(1) to 2.06(1) Å).[50] In the NCN units of the amidinate ligands, the narrow range of the C–N bond lengths (1.320(6) to 1.344(6) Å) confirms the negative charge delocalization in the coordinated anions. The coordination environment around each Cr atom can be regarded as square-planar [angles N(1)–Cr(1)–N(3) 91.9(2)°, N(1)–Cr(1)–N(5) 171.1(1)°, N(1)–Cr(1)–N(7) 87.9(2)°, N(2)–Cr(2)–N(4) 91.5(2)°, N(2)–Cr(2)–N(6) 171.1(1)°, N(2)–Cr(2)–N(8) 87.8(2)°] with each chromium atom slightly elevated above the plane defined by the four nitrogen atoms [Cr(2)–Cr(1)–N(7) 94.3(1), Cr(1)–Cr(2)–N-N(8) 94.5(1)]. For his type of paddle-wheel complexes, the

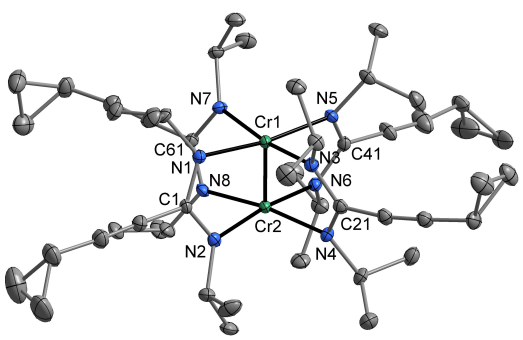

Figure 5. Molecular structure of compound **6** in the crystalline state. Displacement ellipsoids with 40% probability, H atoms omitted for clarity.

Research Article
doi.org/10.1002/ejic.202300027

Cr–Cr bond length can vary over a range of more than 0.7 Å. One of the shortest quadruple bonds is 1.828 (2) Å for $Cr_2[C_6H_3Me(OMe)]_4$ ($C_6H_3Me(OMe)$ = 2-methoxy-5-methylphenyl) whereas Cr–Cr bond lengths of 2.4 Å or more are commonly found in dichromium complexes with axial ligands such as $Cr_2[(2,6\text{-xylyl})\text{-}NC(O)Me]_4\}\cdot 3THF$ (2.221(3) Å).[51,52] The presence of additional ligands in axial positions lengthens the Cr–Cr distances.[53] Generally, Cr–Cr bond lengths of less than 2.0 Å are commonly regarded as very short. The Cr–Cr bond length in the unsolvated complex **6** is 1.889(1) Å, which belongs to the family of the quadruply-bonded dichromium complexes with a very short intermetallic contact such as the related amidinate complex $Cr_2[HC(NCy)_2]_4$ (1.913(3) Å).[50] In rare cases, the bridging coordination mode is not the only interaction involved in stabilizing of the quadruply-bonded dichromium unit, as reported for the homoleptic dichromium amidinate complex $Cr_2[MeC(NtBu)(NEt)]_4$ (1.960(1) Å). In this compound each Cr atom is bonded to the N atoms of one amidinate ligand in a terminal, chelating κ^2N,N'-mode, and to the N atoms of the other two amidinate ligands in a $\kappa N{:}\kappa N'$-bridging mode.[54]

The molecular structure of the dimolybdenum(II) complexes **7** is depicted in Figure 6, while the crystallographic data are summarized in Table 1. Similarly as the Cr complex **6**, the Mo species **7** belong to the same group of paddle wheel-type complexes comprising a central, dinuclear Mo–Mo unit. The two $\kappa O{:}\kappa O'$-acetate and two $\kappa N{:}\kappa N'$-amidinate ligands are in a *trans* arrangement. The Mo–Mo bond length (2.076(1) Å) is consistent with the presence of a Mo–Mo quadruple bond (2.06 to 2.17 Å).[48] The Mo–N bonds range from 2.123(3) to 2.127(3) Å, while the Mo–O distances are in the range of 2.105(2) to 2.121(2) Å, which is slightly shorter than those in the previously published 3 : 1 complexes $Mo_2(ambt)_3(OAc)\cdot 2THF$ (ambt = anion of 2-amino-4-methylbenzothiazole) and $Mo_2[MeC(NPh)_2]_3(OAc)$ (2.16(1) Å in both cases) which comprise amidinate ligands in *trans*-position to the acetate ligand. It was suggested that the increase in the Mo–O(OAc) bond lengths was a manifestation of the *trans*-effect in the latter two molecules.[55,56] The molecular structure of **8** was also elucidated by single crystal X-ray diffraction, but the crystal quality did not allow for full structure refinement. Complex **8** is structurally closely related to **7**, comprising a Mo–Mo core together with three $\kappa N{:}\kappa N'$-amidinate ligands and one $\kappa O{:}\kappa O'$-acetate ligand (cf. Figure S23 in the Supporting Information). A series of other mixed-ligand dimolybdenum(II) acetate/amidinate complexes have been reported earlier, for example $Mo_2[PhC(NSiMe_3)_2]_2(OAc)_2$, $Mo_2[MeC(N^iPr)_2]_2(OAc)_2$, $Mo_2[MeC(N^iPr)_2]_3(OAc)$, and $Mo_2[MeC(NPh)_2]_3(OAc)$.[57,58]

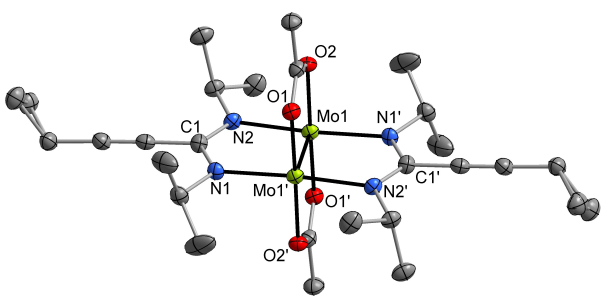

Figure 6. Molecular structure of compound **7** in the crystalline state (one of two molecules in the asymmetric unit). Displacement ellipsoids with 40 % probability, H atoms omitted for clarity. The molecule exhibits crystallographically imposed inversion symmetry. Symmetry code to generate equivalent atoms: ′2−*x*, −*y*, −*z*.

Conclusion

In summary, we succeeded in the preparation and full characterization of two series of new transition metal alkynylamidinates terminated by cyclopropyl groups. The results show that this type of anionic nitrogen ligands is suitable for stabilizing dinuclear complexes of first and second row transition metals ranging from species without significant metal-metal bonding to those comprising Cr–Cr and Mo–Mo quadruple bonds. In view of the ease of preparation of the Li precursors, the new ligand system certainly deserves further exploration. We assume that the alkynylamidinate ligands will play a more significant role in future studies, for example in the exploration of the catalytic activity of metal alkynylamidinate complexes or derivative chemistry involving the –C≡C– triple bond.

Experimental Section

Materials and Methods: All reactions were carried out in oven-dried or flame-dried glassware in an inert atmosphere of dry argon employing standard Schlenk and glovebox techniques. The solvent THF was distilled from sodium/benzophenone in a nitrogen atmosphere prior to use. Transition metal chlorides, *n*-butyllithium (1.6 M in hexanes) and cyclopropylacetylene were purchased from Sigma-Aldrich and used as received. Dichromium(II) tetraacetate and dimolybdenum(II) tetraacetate, $M_2(OAc)_4$ (M = Cr, Mo), were freshly prepared according to the literature procedures.[46,47,59,60] ^{1}H NMR (400 MHz) and ^{13}C NMR (100.6 MHz) spectra were recorded in THF-d_8 solutions using a Bruker DPX 400 spectrometer at 298 K. Chemical shifts are referenced to tetramethylsilane. IR spectra were measured with a Bruker Vertex 70 V spectrometer equipped with a diamond ATR unit between 4000 and 50 cm^{-1}. The relative intensities of the absorption bands are given as very strong (vs), strong (s), medium (m), and weak (w). Unpolarized Raman spectra from 50 to 2500 cm^{-1} in back scattering geometry were measured under using a Raman microscope setup. The collected Raman signal was dispersed by a grating monochromator and recorded by a Peltier cooled charge coupled device camera. An excitation wavelength of 532 nm by employing a doubled YAG:Nd laser was used. All spectra were recorded without using a polarization analyzer. Electron impact (EI) mass spectra were measured on a MAT95 spectrometer with an ionization energy of 70 eV. Microanalyses (C, H, N) of the compounds were performed using a vario EL cube apparatus from Elementar Analysensysteme GmbH. The single-crystal X-ray intensity data were collected on a STOE IPDS 2T diffractometer equipped with a 34 cm image-plate detector, using Mo–K_α radiation. The crystal structures were solved with SHELXT-2018/3[61] and refined by full matrix least-squares methods on F^2 with SHELXL-2018/3[62] using the Olex 1.2 environment.[63] Numerical or spherical absorption correction was applied to the intensity data

for **4a**, **6**, and **7**.[64] CCDC 2226417–2226422 contain the supplementary crystallographic data for this paper (see Table 1). These data can be obtained free of charge from The Cambridge Crystallographic Data Centre (CCDC; http://www.ccdc.cam.ac.uk).

*Preparation of $Mn_2[c\text{-}C_3H_5\text{–}C{\equiv}C\text{–}C(NCy)_2]_4$ (**3**)*: A solution of anhydrous $MnCl_2$ (0.18 g, 1.4 mmol) in 30 mL of THF was added to a solution of **2** (1.0 g, 3.6 mmol) in 50 mL of THF. The reaction mixture was stirred at r.t. for 3 h. The solvent was then removed under vacuum followed by extraction with *n*-pentane (2×30 mL). After a white precipitate (LiCl) was filtered off, the clear, yellow-brown filtrate was concentrated to a total volume of *ca.* 10 mL. An analytically pure crystalline sample was obtained by crystallization from *n*-hexane at 5 °C for one week. The supernatant solution was removed with a cannula and the resulting product was dried under reduced pressure to afford **3** as yellow, prism-like crystals. Yield: 0.49 g (59 %). Mp. 165 °C (dec.). Elem. anal. calcd. for $C_{72}H_{108}Mn_2N_8$ (M = 1195.58 g/mol): C 72.33, H 9.11, N 9.37; found: C 72.27, H 9.36, N 8.70 %. **IR** (ATR): ν = 3655 w, 3442 w, 3232 w, 3093 w, 3011 w, 2921 m, 2848 m (ν C–H), 2663 w, 2623 w, 2581 w, 2225 m (ν C≡C), 1607 m (ν NCN), 1482 vs, 1447 s, 1419 m, 1358 m, 1343 m, 1303 w, 1255 w, 1212 w, 1175 w, 1119 w, 1070 m, 1052 w, 1028 w, 971 m, 922 w, 888 w, 859 w, 842 w, 809 w, 730 w, 693 m, 678 m, 624 m, 590 w, 548 w, 504 w, 431 w, 370 m, 324 m, 282 m, 209 m, 118 w, 164 w, 118 w, 103 w, 80 m cm^{-1}. **MS** (EI, 70 eV): *m/z* (rel. int. %) = 925 (3) [M-(*c*-C_3H_5–C≡C–$C(NCy)_2$)]$^+$, 899 (37) [M-2(*c*-C_3H_5–C≡C)-2(Cy)]$^+$, 667 (100) [M-3(*c*-C_3H_5–C≡C)-4(Cy)]$^+$.

*Preparation of $Fe_2[c\text{-}C_3H_5\text{–}C{\equiv}C\text{–}C(N^iPr)_2]_4$ (**4a**)*: In a fashion similar to the preparation of **3**, reaction of **1** (1.0 g, 3.6 mmol) with anhydrous $FeCl_2$ (0.23 g, 1.8 mmol) afforded **4a** in the form of bright yellow, prism-like crystals. Yield: 0.39 g (49 %). Mp. 165 °C (dec.). Elem. anal. calcd. for $C_{48}H_{76}Fe_2N_8$ (M = 876.88 g/mol): C 65.75, H 8.74, N 12.78; found: C 65.70, H 8.67, N 12.79 %. **IR** (ATR): ν = 3187 w, 3099 w, 3017 w, 2958 vs (ν C–H), 2925 vs (ν C–H), 2861 m (ν C–H), 2800 w, 2708 w, 2618 w, 2599 w, 2218 vs (ν C≡C), 1610 m (ν NCN), 1464 vs, 1425 s, 1376 s, 1344 m, 1328 vs, 1213 m, 1173 vs, 1131 s, 1039 m, 1119 m, 1087 w, 1051 m, 1028 m, 966 vs, 878 w, 843 w, 830 w, 811 m, 744 w, 723 m, 703 m, 690 s, 534 m, 510 w, 485 w, 470 m, 424 m cm^{-1}. **MS** (EI, 70 eV): *m/z* (rel. int. %) = 877 (1) [M]$^+$, 704 (3) [M-4 ^{i}Pr]$^+$, 177 (96) [*c*-C_3H_5–C≡C–C(N^{i}Pr)$_2$–CH_3]$^+$.

*Preparation of $Fe_2[c\text{-}C_3H_5\text{–}C{\equiv}C\text{–}C(NCy)_2]_4$ (**4b**)*: In a fashion similar to the preparation of **3**, reaction of **2** (1.0 g, 2.6 mmol) with anhydrous $FeCl_2$ (0.16 g, 1.3 mmol) afforded **4b** in the form of orange, block-like crystals. Yield: 0.30 g (39 %). Mp. 165 °C (dec.). Elem. anal. calcd. For $C_{75}H_{115}Fe_2N_8$ (M = 1197.40 g/mol): C 72.22, H 9.09, N 9.36; found: C 72.81, H 9.47, N 9.03 %. **IR** (ATR): ν = 3437 w, 3092 w, 3011 w, 2922 vs (ν C–H), 2848 s (ν C–H), 2664 w, 2590 w, 2219 m (ν C≡C), 1689 w, 1605 m (ν NCN), 1466 vs, 1492 vs, 1446 vs, 1394 m, 1361 vs, 1344 s, 1306 m, 1255 m, 1243 w, 1208 w, 1174 m, 1155 m, 1117 m, 1087 w, 1068 m, 1051 m, 1028 m, 971 s, 923 m, 889 m, 858 m, 843 w, 808 m, 734 m, 717 w, 696 m, 676 m, 611 m, 591 m, 552 w, 505 w, 496 w, 480 w, 445 w, 431 w, 389 m, 359 m, 333 w, 303 m, 281 m, 249 s, 219 m, 185 w, 167 w, 120 w, 98 w, 85 w, 73 w, 58 w cm^{-1}. **MS** (EI, 70 eV): *m/z* (rel. int. %) = 899 (1) [M-2(*c*-C_3H_5–C≡C)-2(Cy)]$^+$, 816 (15) 3[*c*-C_3H_5–C≡C–$C(NCy)_2$]$^+$, 636 (43) [M-*c*-C_3H_5–(*c*-C_3H_5–C≡C–$C(NCy)_2$)-3(Cy)]$^+$, 569 (75) [M-2(*c*-C_3H_5–C≡C–C-$(NCy)_2$)–Cy]$^+$.

*Preparation of $Co_2[c\text{-}C_3H_5\text{–}C{\equiv}C\text{–}C(N^iPr)_2]_4$ (**5**)*: In a fashion similar to the preparation of **3**, treatment of **1** (1.0 g, 3.6 mmol) with anhydrous $CoCl_2$ (0.23 g, 1.8 mmol) afforded **5** in the form of yellow-green plate-like crystals. Yield: 0.40 g (50 %). Mp. 116 °C (dec.). Elem. anal. calcd. for $C_{48}H_{76}Co_2N_8$ (M = 883.08 g/mol): C 65.29, H 8.67, N 12.69; found: C 64.71, H 8.50, N 12.43 %. **IR** (ATR): ν = 3685 w, 3096 w, 3014 w, 2959 s (ν C–H), 2923 m (ν C–H), 2866 m (ν C–H), 2707 w, 2616 w, 2219 m (ν C≡C), 1668 w, 1644 w, 1597 m (ν NCN), 1476 vs, 1395 s, 1376 s, 1358 s, 1335 s, 1320 m, 1226 w, 1212 w, 1171 s, 1133 s, 1124 m, 1087 w, 1050 m, 1028 m, 969 s, 876 w, 842 m, 810 m, 719 m, 692 m, 616 w, 573 m, 527 m, 467 m, 420 m, 353 w, 295 m, 259 m, 239 m, 175 m, 104 m, 71 w, 64 w cm^{-1}. **MS** (EI, 70 eV): *m/z* (rel. int. %) = 899 (2) [M + CH_3]$^+$, 667 (5) [M–5 ^{i}Pr]$^+$, 593 (95) [M-3^{i}Pr-4(*c*-C_3H_5)], 501 (62) [M-2(*c*-C_3H_5–C≡C–C-(N^{i}Pr)$_2$)]$^+$.

*Preparation of $Cr_2[c\text{-}C_3H_5\text{–}C{\equiv}C\text{–}C(N^iPr)_2]_4$ (**6**)*: A solution of anhydrous $CrCl_2$ (0.21 g, 1.7 mmol) in 30 mL of THF was added to a solution of **2** (1.0 g, 3.3 mmol) in 50 mL of THF. The reaction mixture was stirred at r.t. overnight. The solvent was removed under vacuum followed by extraction with *n*-pentane (3×20 mL) which produced an orange solution and a white precipitate (LiCl). After filtration and concentration to a total volume of *ca.* 10 mL, an analytical sample was grown by crystallization from *n*-pentane at 5 °C for 5 d. The solvent was decanted with a cannula and the resulting product was dried under reduced pressure to afford **6** in the form of orange, rod-like crystals. Yield: 0.29 g (41 %). A 60 % isolated yield was obtained when $Cr_2(OAc)_4$ was treated under the same conditions with 4 equiv. of **2**. Mp. 146 °C (dec.). Elem. anal. calcd. for $C_{48}H_{76}Cr_2N_8$ (M = 869.16 g/mol): C 66.33, H 8.81, N 12.89; found: C 66.41, H 8.50, N 12.43 %. **IR** (ATR): ν = 3086 w, 2964 m (ν C–H), 2921 m, 2867 m (ν C–H), 2610 w, 2221 m (ν C≡C), 1984 w, 1694 w, 1638 w, 1562 w, 1506 vs (ν NCN), 1491 vs, 1447 m, 1414 s, 1373 s, 1354 s, 1318 s, 1246 w, 1222 w, 1199 m, 1179 s, 1163 w, 1145 m, 1123 s, 1110 s, 1051 m, 1027 m, 974 vs, 932 m, 864 m, 845 m, 810 m, 746 m, 697 s, 660 w, 621 m, 612 w, 598 m, 553 m, 507 m, 463 m, 427 m, 388 w, 324 w, 275 m, 249 w, 204 w, 157 m, 150 m, 117 w, 104 w, 94 w, 63 w, 54 w cm^{-1}. **^{1}H NMR** (400 MHz, THF-d_8, 25 °C): δ = 3.75 (br s, 8 H, C*H*(CH$_3$)$_2$), 1.46–1.53 (m, 4 H, C*H*, *c*-C_3H_5), 1.42 (d, 24 H, CH(C*H*$_3$)$_2$), 0.98 (br, 24 H, CH(C*H*$_3$)$_2$), 0.76–0.89 (m, 16 H, C*H*$_2$, *c*-C_3H_5) ppm. **^{13}C NMR** (100.6 MHz, THF-d_8, 25 °C): δ = 156.3 (N*C*N), 96.9 (CH$_2$–*C*≡C), 72.6 (C≡*C*–C), 51.7 (*C*H(CH$_3$)$_2$), 24.3 (CH-(*C*H$_3$)$_2$), 23.5 (CH(*C*H$_3$)$_2$), 8.3 (*C*H$_2$, *c*-C_3H_5), 8.1 (*C*H$_2$, *c*-C_3H_5), 0.6 (*C*H, *c*-C_3H_5) ppm. **MS** (EI, 70 eV): *m/z* (rel. int. %) = 869 (35) [M]$^+$, 626 (50) [M-3^{i}Pr-2N^{i}Pr]$^+$, 554 (35) [M-3(*c*-C_3H_5)–(*c*-C_3H_5–C≡C–C(N^{i}Pr)$_2$)]$^+$, 478 (100) [M-4(*c*-C_3H_5–C≡C)–3^{i}Pr]$^+$.

*Preparation of $Mo_2[c\text{-}C_3H_5\text{–}C{\equiv}C\text{–}C(N^iPr)_2]_2(OAc)_2$ (**7**)*: In a fashion similar to the preparation of **6**, reaction of **1** (1.0 g, 3.6 mmol) with anhydrous $Mo_2(OAc)_4$ (0.77 g, 1.8 mmol) afforded **7** in the form of orange, block-like crystals. Yield: 0.81 g (65 %). Mp. 191 °C (dec.). Elem. anal. calcd. for $C_{28}H_{44}Mo_2N_4O_4$ (M = 692.56 g/mol): C 48.56, H 6.40, N 8.09; found: C 48.56, H 6.42, N 8.17 %. **IR** (ATR): ν = 3093 w, 2963 m (ν C–H), 2945 m, 2921 m, 2865 m (ν C–H), 2606 w, 2216 m (ν C≡C), 1531 s (ν NCN), 1438 vs, 1427 vs, 1375 s, 1356 m, 1333 m, 1207 w, 1172 m, 1138 m, 1122 m, 1086 w, 1052 w, 1027 m, 968 s, 934 w, 872 w, 861 w, 847 w, 809 m, 771 w, 721 w, 695 w, 672 s, 622 w, 596 w, 561 w, 532 w, 507 w, 452 w, 416 w, 366 w, 346 w, 302 s, 271 m, 223 w, 197 w, 190 w, 167 w, 157 w, 145 w, 125 w, 103 w, 86 w, 66 w, 56 w cm^{-1}. **^{1}H NMR** (400 MHz, THF-d_8, 25 °C): δ = 4.57 (sept, 4 H, C*H*(CH$_3$)$_2$), 2.29 (s, 6 H, O$_2$CCH$_3$), 1.55–1.61 (m, 2 H, C*H*, *c*-C_3H_5), 0.79 (d, 24 H, CH(C*H*$_3$)$_2$), 0.78–0.95 (m, 8 H, C*H*$_2$, *c*-C_3H_5) ppm. **^{13}C NMR** (100.6 MHz, THF-d_8, 25 °C): δ = 148.0 (N*C*N), 95.4 (CH–*C*≡C), 70.3 (C≡*C*–C), 68.5 (C≡*C*–C), 58.0 (O$_2$*C*CH$_3$), 53.7 (CH-(*C*H$_3$)$_2$), 53.4 (*C*H(CH$_3$)$_2$), 25.1 (CH(*C*H$_3$)$_2$), 23.2 (CH(*C*H$_3$)$_2$), 22.9 (O$_2$C*C*H$_3$), 9.1 (*C*H$_2$, *c*-C_3H_5), 80.15 (*C*H, *c*-C_3H_5) ppm. **MS** (EI, 70 eV): *m/z* (rel. int. %) = 692 (100) [M]$^+$, 501 (6) [M-(*c*-C_3H_5–C≡C–C-(N^{i}Pr)$_2$)]$^+$.

*Preparation of $Mo_2[c\text{-}C_3H_5\text{–}C{\equiv}C\text{–}C(N^iPr)_2]_3(OAc)$ (**8**)*: In a fashion similar to the preparation of **6**, treatment of anhydrous $Mo_2(OAc)_4$ (0.51 g, 1.2 mmol) with **1** (1.0 g, 3.6 mmol, 3 equiv.) afforded **8** in the form of yellow block-like crystals. Yield: 0.31 g (30 %). Mp. 185 °C (dec.). Elem. anal. calcd. for $C_{38}H_{60}Mo_2N_6O_2$ (M = 824.81 g/mol): C 55.34, H 7.33, N 10.19; **IR** (ATR): ν = 3188 w, 3078 w, 3007 w, 2971 m (ν C–H), 2930 w (ν C–H), 2875 w (ν C–H), 2728 w, 2227 m (ν

C≡C), 2164 w, 2148 w, 2122 w, 1995 w, 1896 w, 1627 vs (ν NCN), 1566 vs, 1442 m, 1428 m, 1389 m, 1371 m, 1326 m, 1280 m, 1210 w, 1167 m, 1128 s, 1086 w, 1055 w, 1030 w, 978 m, 968 w, 932 m, 890 s, 867 s, 784 m, 761 m, 737 m, 667 m, 614 w, 606 w, 571 w, 521 w, 450 w, 429 w, 409 w, 348 w, 315 w, 301 w, 297 w, 267 w, 195 w, 159 w, 148 w, 122 m, 110 m, 97 w, 80 w, 68 w, 54 w cm^{-1}. **^{1}H NMR** (400 MHz, THF-d_8, 25 °C): δ = 4.59 (sept, 2H, C*H*(CH$_3$)$_2$), 4.48 (sept, 2H, C*H*(CH$_3$)$_2$), 3.82–3.74 (m, 2H, C*H*(CH$_3$)$_2$), 2.30 (s, 3 H, O$_2$CCH$_3$), 1.54–1.62 (m, 3 H, C*H*, *c*-C$_3$H$_5$), 1.49 (d, 6H, CH(C*H*$_3$)$_2$), 1.16 (d, 6H, CH(C*H*$_3$)$_2$), 1.02 (d, 9H, CH(C*H*$_3$)$_2$), 0.83–0.94 (m, 12H, C*H*$_2$, *c*-C$_3$H$_5$; 15 H, CH(C*H*$_3$)$_2$ ppm. **^{13}C NMR** (100.6 MHz, THF-d_8, 25 °C): δ = 149.0, 148.1, (N*C*N), 95.2, 94.8 (CH–*C*≡C), 70.3, 69.7 (C≡*C*–C), 57.8 (O$_2$*C*CH$_3$), 54.0, 53.7, 51.8 (*C*H(CH$_3$)$_2$), 24.8, 23.9, 23.5, 23.2, 23.1 (CH(*C*H$_3$)$_2$), 21.9 (O$_2$CCH$_3$), 8.93, 8.90, 8.87 (*C*H$_2$, *c*-C$_3$H$_5$), 0.51, 0.34, 0.21 (*C*H, *c*-C$_3$H$_5$) ppm. **MS** (EI, 70 eV): *m/z* (rel. int. %) = 828 (88) [M]$^+$, 692 (100) [M-(*c*-C$_3$H$_5$–C≡C)-*c*-C$_3$H$_5$-2CH$_3$]$^+$.

Deposition Numbers 2226417 (for **3**·0.5 *n*-C$_6$H$_{14}$), 2226418 (for **4a**), 2226419 (for **4b**), 2226420 (for **5**), 2226421 (for **6**), 2226422 (for **7**) contain the supplementary crystallographic data for this paper. These data are provided free of charge by the joint Cambridge Crystallographic Data Centre and Fachinformationszentrum Karlsruhe Access Structures service.

Acknowledgements

S.W. acknowledges the award of a PhD scholarship from the China Scholarship Council (CSC) (File No. 201508080111). We also thank the Otto-von-Guericke-Universität Magdeburg for general financial support. Open Access funding enabled and organized by Projekt DEAL.

Conflict of Interest

The authors declare no conflict of interest.

Data Availability Statement

The data that support the findings of this study are available from the corresponding author upon reasonable request.

Keywords: alkynylamidinate · amidinate · lithium · multiple bonds · transition metal · X-ray diffraction

[1] W. E. Piers, D. J. H. Emslie, *Coord. Chem. Rev.* **2002**, *233–234*, 131–155.
[2] P. Braunstein, *Chem. Rev.* **2006**, *106*, 134–159.
[3] A. A. Trifonov, *Coord. Chem. Rev.* **2010**, *254*, 1327–1347.
[4] C. Fliedel, A. Ghisolfi, P. Braunstein, *Chem. Rev.* **2016**, *116*, 9237–9304.
[5] F. T. Edelmann, *Chem. Soc. Rev.* **2009**, *38*, 2253–2268.
[6] F. T. Edelmann, *Chem. Soc. Rev.* **2012**, *41*, 7657–7672.
[7] P. Buchwalter, J. Rosé, P. Braunstein, *Chem. Rev.* **2015**, *115*, 28–126.
[8] C. Zovko, S. Bestgen, C. Schoo, A. Görner, J. M. Goicoechea, P. W. Roesky, *Chem. Eur. J.* **2020**, *26*, 13191–13202.
[9] M. P. Coles, P. B. Hitchcock, *Chem. Commun.* **2002**, 2794–2795.
[10] N. Tsukada, O. Tamura, Y. Inoue, *Organometallics* **2002**, *21*, 2521–2528.
[11] Z. Feng, Y. Jiang, H. Ruan, Y. Zhao, G. Tan, L. Zhang, X. Wang, *Dalton Trans.* **2019**, *48*, 14975–14978.
[12] P. C. Junk, M. L. Cole, *Chem. Commun.* **2007**, 1579–1590.
[13] F. T. Edelmann, *Adv. Organomet. Chem.* **2008**, *57*, 183–352.
[14] C. E. Hayes, D. B. Leznoff, *Coord. Chem. Rev.* **2014**, *266–267*, 155–170.
[15] Y.-Y. Zhang, Y.-J. Lin, X.-C. Shi, G.-X. Jin, *Pure Appl. Chem.* **2014**, *86*, 953–965.
[16] T. Chlupatý, A. Růžička, *Coord. Chem. Rev.* **2016**, *314*, 103–113.
[17] G. B. Deacon, M. E. Hossain, P. C. Junk, M. Salehisaki, *Coord. Chem. Rev.* **2017**, *340*, 247–265.
[18] B. E. Bursten, M. H. Chisholm, R. J. H. Clark, S. Firth, C. M. Hadad, P. J. Wilson, P. M. Woodward, J. M. Zaleski, *J. Am. Chem. Soc.* **2002**, *124*, 12244–12254.
[19] M. H. Chisholm, *Dalton Trans.* **2003**, 3821–3828.
[20] F. R. Wagner, A. Noor, R. Kempe, *Nat. Chem.* **2009**, *1*, 529–536.
[21] A. Noor, G. Glatz, R. Müller, M. Kaupp, S. Demeshko, R. Kempe, *Z. Anorg. Allg. Chem.* **2009**, *635*, 1149–1152.
[22] N. V. S. Harisomayajula, A. K. Nair, Y.-C. Tsai, *Chem. Commun.* **2014**, *50*, 3391–3412.
[23] W.-W. Zhang, M. Nishiura, Z. Hou, *J. Am. Chem. Soc.* **2005**, *127*, 16788–16789.
[24] S. Zhou, S. Wang, G. Yang, Q. Li, L. Zhang, Z. Yao, Z. Zhou, H.-B. Song, *Organometallics* **2007**, *26*, 3755–3761.
[25] W.-X. Zhang, Z. Hou, *Org. Biomol. Chem.* **2008**, *6*, 1720–1730.
[26] Z. Du, W. Li, X. Zhu, F. Xu, Q. Shen, *J. Org. Chem.* **2008**, *73*, 8966–8972.
[27] M. Li, S. Fang, J. Zheng, H. Jiang, W. Wu, *Org. Lett.* **2019**, *21*, 8439–8443.
[28] Y. Wu, S. Wang, L. Zhang, G. Yang, X. Zhu, Z. Zhou, H. Zhu, S. Wu, *Eur. J. Org. Chem.* **2010**, 326–332.
[29] F. Zhang, J. Zhang, Y. Zhang, J. Hong, X. Zhou, *Organometallics* **2014**, *33*, 6186–6192.
[30] T. J. Feuerstein, M. Po, T. P. Seifert, S. Bestgen, C. Feldmann, P. W. Roesky, *Chem. Commun.* **2017**, *53*, 9012–9015.
[31] P. Dröse, C. G. Hrib, F. T. Edelmann, *J. Organomet. Chem.* **2010**, *695*, 1953–1956.
[32] L. Xu, Y.-C. Wang, W.-X. Zhang, Z. Xi, *Dalton Trans.* **2013**, *42*, 16466–16469.
[33] W. W. Seidel, W. Dachtler, T. Pape, *Z. Anorg. Allg. Chem.* **2012**, *638*, 116–121.
[34] A. de Meijere, S. I. Kozhushkov, *Mendeleev Commun.* **2010**, *20*, 301–311.
[35] D. Dulov, O. Levitskiy, A. Bogdanov, T. Magdesieva, *ChemistrySelect* **2021**, *6*, 9653–9656.
[36] F. M. A. Sroor, C. G. Hrib, L. Hilfert, F. T. Edelmann, *Z. Anorg. Allg. Chem.* **2013**, *639*, 2390–2394.
[37] F. M. A. Sroor, C. G. Hrib, L. Hilfert, P. G. Jones, F. T. Edelmann, *J. Organomet. Chem.* **2015**, *785*, 1–10.
[38] F. M. A. Sroor, C. G. Hrib, L. Hilfert, S. Busse, F. T. Edelmann, *New J. Chem.* **2015**, *39*, 7595–7601.
[39] F. M. A. Sroor, C. G. Hrib, L. Hilfert, L. Hartenstein, P. W. Roesky, F. T. Edelmann, *J. Organomet. Chem.* **2015**, *799–800*, 160–165.
[40] F. M. A. Sroor, C. G. Hrib, P. Liebing, L. Hilfert, S. Busse, F. T. Edelmann, *Dalton Trans.* **2016**, *45*, 13332–13346.
[41] S. Wang, F. M. Sroor, P. Liebing, V. Lorenz, L. Hilfert, F. T. Edelmann, *Acta Crystallogr.* **2016**, *E72*, 1229–1233.
[42] S. Wang, P. Liebing, F. Engelhardt, L. Hilfert, S. Busse, F. T. Edelmann, *Acta Crystallogr.* **2018**, *E74*, 1658–1664.
[43] S. Wang, P. Liebing, F. Engelhardt, L. Hilfert, S. Busse, R. Goldhahn, F. T. Edelmann, *Z. Anorg. Allg. Chem.* **2022**, *648*, e202200009.
[44] S. Wang, P. Liebing, F. Engelhardt, L. Hilfert, S. Busse, R. Goldhahn, F. T. Edelmann, *Z. Anorg. Allg. Chem.* **2023**, *649*, e202200289.
[45] J. Richter, J. Feiling, H.-G. Schmidt, M. Noltemeyer, W. Brüser, F. T. Edelmann, *Z. Anorg. Allg. Chem.* **2004**, *630*, 1269–1275.
[46] S. N. Setkar, M. Fink, *J. Am. Chem. Soc.* **1985**, *107*, 338–340.
[47] F. A. Cotton, Z. C. Mester, T. R. Webb, *Acta Crystallogr.* **1974**, *B30*, 2768–2770.
[48] R. E. Da Re, J. L. Eglin, C. N. Carlson, K. D. John, D. E. Morris, W. H. Woodruff, J. A. Bailey, E. Batista, R. L. Martin, F. A. Cotton, E. A. Hillard, C. A. Murillo, A. P. Sattelberger, R. J. Donohue, *J. Am. Chem. Soc.* **2010**, *132*, 1839–1847.
[49] F. A. Cotton, L. M. Daniels, J. H. Matonic, C. A. Murillo, *Inorg. Chim. Acta* **1997**, *256*, 277–282.
[50] H. Shoukang, S. Gambarotta, C. Bensimon, J. J. H. Edema, *Inorg. Chim. Acta* **1993**, *213*, 65–74.
[51] F. A. Cotton, S. A. Koch, M. Millar, *Inorg. Chem.* **1978**, *17*, 2084–2086.
[52] F. A. Cotton, W. H. Ilsley, W. Kaim, *J. Am. Chem. Soc.* **1980**, *102*, 3464–3474.
[53] F. A. Cotton, C. A. Murillo, I. Pascual, *Inorg. Chem.* **1999**, *38*, 2182–2187.
[54] A. R. Sadique, M. J. Heeg, C. H. Winter, *J. Am. Chem. Soc.* **2003**, *125*, 7774–7775.
[55] F. A. Cotton, W. H. Ilsley, W. Kaim Inorg, *Chem.* **1981**, *20*, 930–934.

Research Article
doi.org/10.1002/ejic.202300027

[56] F. A. Cotton, W. H. Ilsley, *Inorg. Chem.* **1981**, *20*, 572–578.
[57] Y. Yamaguchi, S. Ozaki, H. Hinago, K. Kobayashi, T. Ito, *Inorg. Chim. Acta* **2005**, *358*, 2363–2370.
[58] G. Zou, T. Ren, *Inorg. Chim. Acta* **2000**, *304*, 305–308.
[59] O. Levy, B. Bogoslavsky, A. Bino, *Inorg. Chim. Acta.* **2012**, *391*, 179–181.
[60] I. Song, J. Koo, S. M. Yoon, *RSC Adv.* **2019**, *9*, 24319–24324.
[61] G. M. Sheldrick, *Acta Crystallogr.* **2015**, *A71*, 3–8.
[62] G. M. Sheldrick, *Acta Crystallogr.* **2015**, *C71*, 3–8.
[63] O. V. Dolomanov, L. J. Bourhis, R. J. Gildea, J. A. K. Howard, H. Puschmann, *J. Appl. Crystallogr.* **2009**, *42*, 339–341.
[64] Stoe & Cie **2002**, *X-Area, X-Step and X-Red*, Stoe & Cie, Darmstadt, Germany.

Manuscript received: January 13, 2023
Revised manuscript received: March 7, 2023
Accepted manuscript online: March 7, 2023